CHEMISTRY
A European Journal

A Journal of
ChemPubSoc Europe

Accepted Article

Title: Cyclopropane-Based Peptidomimetics Mimicking Wide-Ranging Secondary Structures of Peptides: Conformational Analysis and Their Use in Rational Ligand Optimization

Authors: Akira Mizuno, Tomoshi Kameda, Tomoki Kuwahara, Hideyuki Endoh, Yoshihiko Ito, Shizuo Yamada, Kimiko Hasegawa, Akihito Yamano, Mizuki Watanabe, Mitsuhiro Arisawa, and Satoshi Shuto

To be cited as: *Chem. Eur. J.* 10.1002/chem.201605312

Link to VoR: http://dx.doi.org/10.1002/chem.201605312

Supported by
ACES

WILEY-VCH

10.1002/chem.201605312

WILEY-VCH

Cyclopropane-Based Peptidomimetics Mimicking Wide-Ranging Secondary Structures of Peptides: Conformational Analysis and Their Use in Rational Ligand Optimization

Akira Mizuno,[a] Tomoshi Kameda,[c] Tomoki Kuwahara,[a] Hideyuki Endoh,[a] Yoshihiko Ito,[d] Shizuo Yamada,[d] Kimiko Hasegawa,[e] Akihito Yamano,[e] Mizuki Watanabe,[a] Mitsuhiro Arisawa[a] and Satoshi Shuto*[a,b]

Abstract: Detailed conformational analyses of our previously reported cyclopropane-based peptidomimetics and conformational analysis-driven ligand optimization are described. Computational calculations and X-ray crystallography showed that the characteristic features of cyclopropane function effectively to constrain the molecular conformation in a three-dimensionally diverse manner. Subsequent principal component analysis revealed that the diversity covers the broad chemical space filled by peptide secondary structures in terms of both main-chain and side-chain conformations. Based on these analyses, a lead stereoisomer targeting melanocortin receptors was identified, and its potency and subtype selectivity were improved by further derivatization. The presented strategy is effective not only for designing non-peptidic ligands from a peptide ligand, but also for the rational optimization of these ligands based on the plausible target-binding conformation without requiring the three-dimensional structural information of the target and its peptide ligands.

Introduction

Peptidomimetics, in which natural bioactive peptides are converted into non-peptidic drug-like molecules, are an important concept in modern drug development.[1] The essence of peptidomimetic design is to mimic the secondary structure of a key amino acid sequence in the parent peptide ligand interacting with its target.[2] The rational design and optimization of peptidomimetics, however, are challenging due to the inherent flexibility of peptides. This is especially true when the defined three-dimensional (3D) structural information on the peptide-target interaction is not available, as is often the case when the target is a G protein-coupled receptor (GPCR).[3] Therefore, an effective methodology for designing and optimizing peptidomimetics without 3D structural information of the target and its peptide ligands is strongly needed.

One of the most well-investigated approaches for developing peptidomimetics targeting peptide-protein and peptide-receptor interactions is to mimic the folded secondary structures, such as β-turns, of peptide ligands.[4] This is mainly because a number of bioactive peptides are recognized by the target proteins while in their folded conformations.[5] While promising, however, this approach is often unsuccessful due to the difficulty of mimicking the exact conformations recognized by the target, due to the high conformational diversity of peptide secondary structures.[6] For example, there are more than eight types of β-turn structures, which makes it difficult to predict which β-turn structure is important for binding.[7] Further, in some cases, key amino acid residues interacting with the target protein might assume a more extended conformation than the turn structures.[8] The design of peptidomimetics, therefore, requires the incorporation of "3D structural diversity" to cover the broad array of peptide secondary structures, i.e., from folded to extended forms, including their halfway structures, rather than focusing on mimicking only one of them.

Cyclopropane effectively restricts the conformation of a molecule in the *cis* (folded)- or *trans* (extended)-form as shown in Figure 1a. This structural property, *cis*/*trans*-restriction, is widely used in medicinal chemistry,[9] including the field of peptidomimetics.[10] In addition, cyclopropane has two other characteristic features. First, cyclopropanes directly connected to an sp^2 carbon exist preferentially in the bisected conformation, as shown in Figure 1b, due to the π-donating stereoelectronic effect of the cyclopropane ring.[11] Second, *cis*-configured substituents on a cyclopropane ring mutually exert marked steric repulsion, because they are fixed in the eclipsed form, referred to as cyclopropylic strain.[12] Consequently, the rotational conformation of the substituents on cyclopropane can be

[a] Dr. A. Mizuno, T. Kuwahara, H. Endoh, Dr. M. Watanabe, Dr. M. Arisawa, Prof. Dr. S. Shuto
Faculty of Pharmaceutical Sciences
Hokkaido University
Kita-12, Nishi-6, Kita-ku, Sapporo, Hokkaido 060-0812 (Japan)
E-mail: shu@pharm.hokudai.ac.jp

[b] Prof. Dr. S. Shuto
Center for Research and Education on Drug Discovery
Hokkaido University
Kita-12, Nishi-6, Kita-ku, Sapporo, Hokkaido 060-0812 (Japan)

[c] Dr. T. Kameda
Computational Biology Research Center
National Institute of Advanced Industrial Science and Technology
2-4-7, Aomi, Koutou-ku, Tokyo 135-0064 (Japan)

[c] Dr. Y. Ito, Prof. Dr. S. Yamada
School of Pharmaceutical Sciences
University of Shizuoka
Yata, Suruga-ku, Shizuoka, Shizuoka 422-8526 (Japan)

[d] Dr. K. Hasegawa, Dr. A. Yamano
Rigaku Corporation, Application Laboratories
3-9-12, Matsubara-cho, Akishima, Tokyo 196-8666 (Japan)

Supporting information for this article including full analytical and experimental procedures as well as copies of ^{1}H and ^{13}C NMR data is available on the WWW under http://xxxx

restricted to minimize the steric repulsion due to the strain, as shown in Figure 1c.

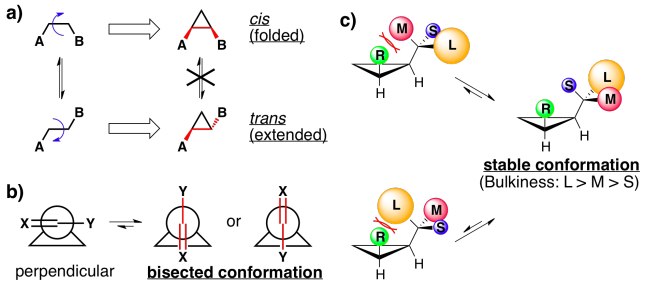

Figure 1. Steric and stereoelectronic features of cyclopropane. (a) *cis/trans*-restriction; (b) bisected conformational-preference; (c) cyclopropylic strain.

We hypothesized that taking advantage of all of these characteristic features of cyclopropane would provide a useful peptidomimetic scaffold with sufficient 3D structural diversity to mimic various peptide secondary structures. As shown in Figure 2, when the central peptide bond moiety of a tetrapeptide motif is replaced with a cyclopropane ring, the conformation of the *i*+2 and *i*+3 moieties can be controlled by the *cis*/*trans*-restriction and the bisected-conformational preference, respectively, and the spatial arrangement of the *i* and *i*+1 moieties can be restricted by the cyclopropylic strain, depending on the stereochemistries of the stereogenic carbon centers. This hypothesis was examined by designing peptidomimetics targeting melanocortin receptors (MCRs), a family of GPCRs. Some of the designed mimetics exhibited the desired binding affinity to the receptor.[13] Whether or not the cyclopropane-based peptidomimetics actually have 3D structural diversity as hypothesized, however, was not experimentally verified, which limited the utility of these mimetics to some extent. For this viewpoint, the 3D structures of the peptidomimetics should be investigated by an appropriate methodology.[14]

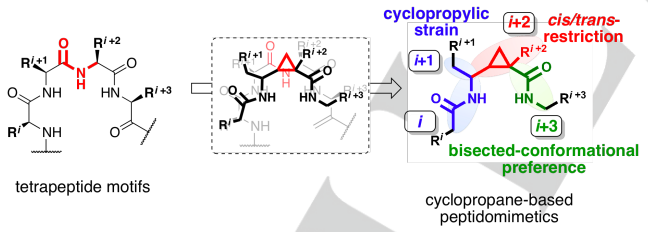

Figure 2. Design of cyclopropane-based peptidomimetics by replacing the middle peptide bond moiety in tetrapeptide motifs with a cyclopropane ring.

Thus, in the present study, we performed conformational analyses of the cyclopropane-based peptidomimetics to clarify whether the mimetics actually cover the broad chemical space filled by the diverse peptide secondary structures in terms of both main-chain and side-chain conformations. Furthermore, we also performed rational ligand optimization based on the conformational analyses. In this optimization process, we investigated the 3D structural information important for the receptor binding, which led to the efficient identification of a more potent and subtype-selective MCR ligand.

Results

Conformational Analyses of the Cyclopropane-Based Peptidomimetics

1) Computational calculations

The designed cyclopropane-based peptidomimetics comprised eight stereoisomers because of the three consecutive asymmetric carbons (Figure 3). The direction of the cyclopropane ring is either up or down. The peptidomimetic backbone (indicated in red in Figure 3) can be fixed to the *cis*- or *trans*-configuration by the ring, and is also constrained to either the extended or folded form by the cyclopropylic strain depending on the stereochemistry of the asymmetric center adjacent to the ring (C1'). The eight stereoisomers were thus named **I** (up/*trans*-folded), **II** (up/*trans*-extended), **III** (up/*cis*-extended), **IV** (up/*cis*-folded), ***ent*-I** (down/*trans*-folded), ***ent*-II** (down/*trans*-extended), ***ent*-III** (down/*cis*-extended), and ***ent*-IV** (down/*cis*-folded).

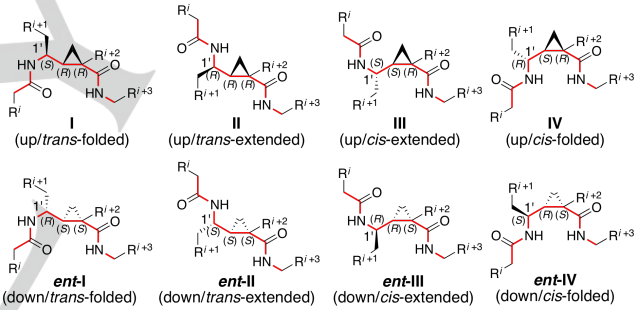

Figure 3. Diagram of the structural difference of the eight stereoisomers in the cyclopropane-based peptidomimetics.

Structural analyses of the four stereoisomers **I**–**IV** were carried out by computational calculations with MacroModel using the simplified models **A** (for **I**, up/*trans*-folded), **B** (for **II**, up/*trans*-extended), **C** (for **III**, up/*cis*-extended), and **D** (for **IV**, up/*cis*-folded), and their most stable conformations are shown in Figure 4. The cyclopropylic strain was observed to be effective in all four stereoisomers. Their backbone conformation was evaluated based on the dα value, which is the distance between the two terminal carbons corresponding to $C\alpha_i$ and $C\alpha_{i+3}$ in a tetrapeptide motif. The dα values obtained were 7.2 Å for **A**, 9.5 Å for **B**, 9.1 Å for **C**, and 6.2 Å for **D**; demonstrating that the backbone conformations were remarkably varied with dα values ranging from 6.2 to 9.5 Å. Thus, the conformational diversity of the peptidomimetic backbone could cover a wide range of peptide secondary structures from β-turns to β-strands.

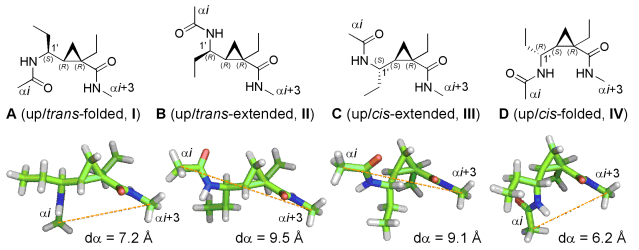

Figure 4. Most stable conformations for models **A**–**D**. The distance between the two terminal carbons (indicated by α_i and α_{i+3}) are shown as dα in each model structure.

2) X-ray Crystallography

To corroborate the above calculation results by X-ray crystallography, the simplified mimetics **A'**–**D'** were designed and synthesized as racemates, considering the crystallinity. As shown in Scheme 1, synthesis was based on stepwise incorporation of the four side-chain moieties (R^i to R^{i+3}) into cyclopropane unit **1**, which we previously established as a general synthetic route.[13] For *trans*-type mimetics, the R^{i+2} moiety was introduced into the lactone carbonyl group of **1**, while the ethoxy group of the ester was replaced with the amine bearing the R^{i+3} moiety. For *cis*-type mimetics, the R^{i+2} moiety was introduced to the ester carbonyl group of **1**, while the lactone was opened with the amine bearing the R^{i+3} moiety. The C1' stereogenic center was constructed via the Grignard reaction, introducing the R^{i+1} moiety to *N-tert*-butanesulfinyl imines **2** and **3**. Finally, the amino group of the Grignard products was coupled with the carboxylic acid bearing the R^i moiety to give the desired mimetics.[15]

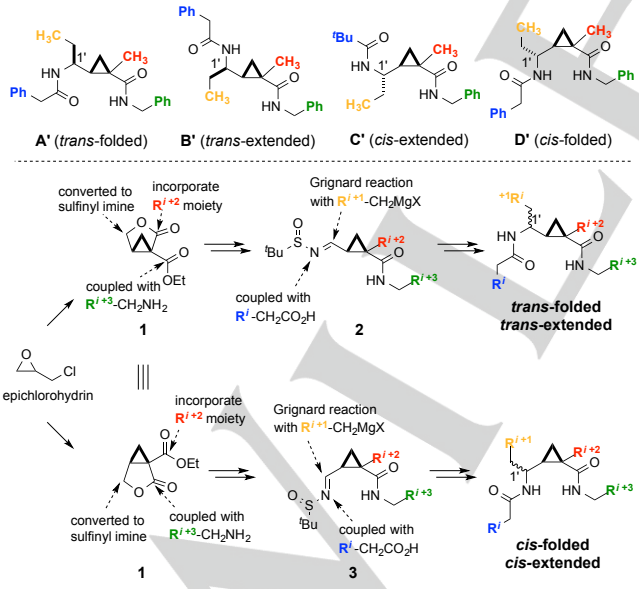

Scheme 1. Structures of compounds **A'**–**D'** designed for X-ray crystallography, and the general synthetic scheme of the cyclopropane-based peptidomimetics.

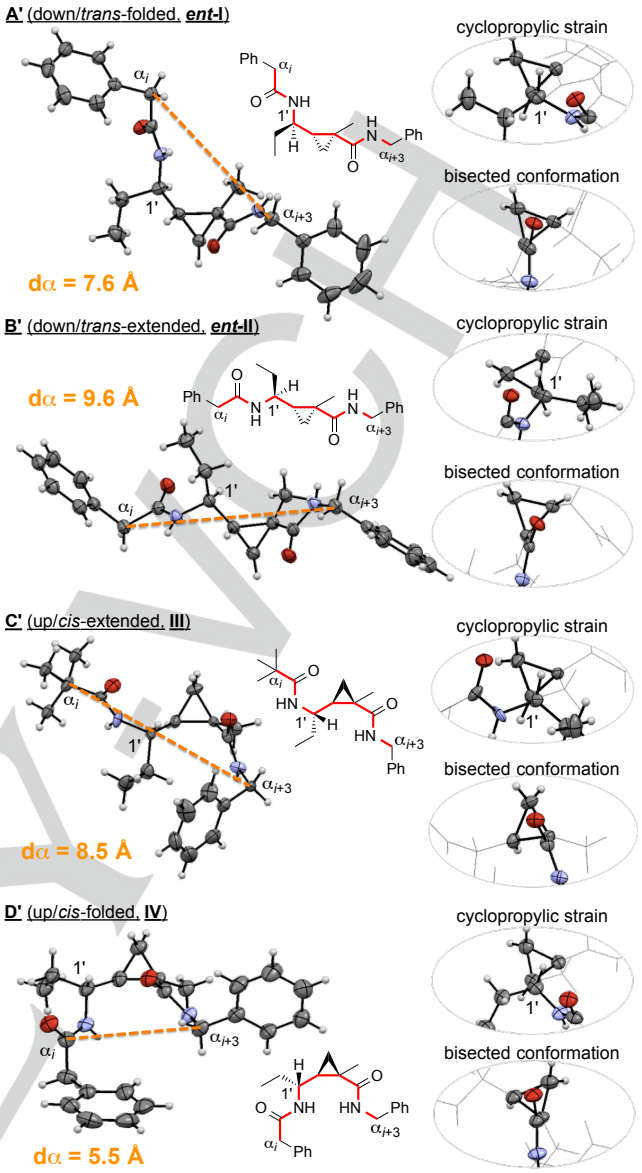

Figure 5. X-ray crystallographic structures of compounds **A'**-**D'**. The conformational restriction due to the cyclopropylic strain and the bisected-conformational preference are highlighted, and the dα value is shown for each crystal structure.

As shown in Figure 5, the X-ray crystal structures showed that both the bisected-conformational preference and the cyclopropylic strain worked effectively to restrict the conformation. Accordingly, the structures were well superimposed on the corresponding calculated structures, i.e., **A** on the *trans*-folded model **A**, **B'** on the *trans*-extended model **B**, **C'** on the *cis*-extended model **C**, and **D'** on the *cis*-folded model **D**, while, in compound **C'**, the amide bond adjacent to the cyclopropane ring rotated by approximately 45° from the ideal bisected conformation, probably due to the steric repulsion against the spatially close ethyl group. The dα values of the crystal structures of the synthesized mimetics **A'**-**D'** were almost

consistent with those calculated for models **A**-**D**, respectively. In addition, the dα value of crystalline **D'** was shorter than that calculated for model **D** by 0.7 Å, suggesting that the peptidomimetic backbone can span to an even broader extent than predicted by the computational calculations.

3) Principal Component Analysis

Peptidomimetic structures must be evaluated not only for the main-chain (backbone) conformation, but also for the side-chain (R^i to R^{i+3}) positioning, due to its major role in the interaction with targets. Accordingly, using the obtained X-ray crystal structures, the peptidomimetics were compared with the diverse secondary structures of tetrapeptide motifs by principal component analysis (PCA), a mathematical method generally used to evaluate the diversity of molecular characteristics.[16]

Considering the range where the conformational restriction of cyclopropane can be effective, the six carbon atoms were selected as the comparison points, which comprised the four α-carbons of the residues *i* to *i*+3 ($C\alpha_i$ to $C\alpha_{i+3}$) and the two β-carbons of the central two residues ($C\beta_{i+1}$ and $C\beta_{i+2}$) indicated by the magenta points in Figure 6a. To build a chemical space that describes the conformational diversity of tetrapeptide motifs, 3D structural data of tetrapeptide motifs (12,410 in total) were extracted from the X-ray crystal structures of peptides deposited in PepX, a peptide-protein complex database.[17] PCA was performed on the 3D coordinates of the six carbon atoms in the extracted tetrapeptide motifs, and the first and second principal components (PC1 and PC2) were used to build the chemical space. As shown in Figure 6b, PC1 (horizontal axis) and PC2 (vertical axis) of each extracted tetrapeptide motif are plotted as red crosses. PC1 clearly correlated with the distance between $C\alpha_i$ and $C\alpha_{i+3}$ (dα in Figure 7; correlation coefficient r = 0.95), while PC2 was weakly to moderately correlated with the distance between $C\beta_{i+1}$ and $C\beta_{i+2}$ (dβ in Figure 7; r = -0.30) and the dihedral angle of $C\beta_{i+1}$-$C\alpha_{i+1}$-$C\alpha_{i+2}$-$C\beta_{i+2}$ (θ in Figure 7; r = -0.55). Based on these structural meanings, PC1 can describe the folded/extended character of the main chain, while PC2 indicates the 3D positioning of the side chains of the central two residues *i*+1 and *i*+2. Therefore, the broadly distributed red plots in the chemical space shown in Figure 6b clearly demonstrate that the conformations of the tetrapeptide motifs in PepX are diverse in terms of both main-chain conformation and side-chain positioning.

The corresponding six carbon atoms in the cyclopropane-based peptidomimetics were also selected for the PCA (Figure 6a, magenta points). PC1 and PC2, calculated based on the X-ray crystal structures of the compounds **A'**–**D'**, corresponding to the eight scaffolds **I**–**IV** and ***ent*-I**–**IV**, are plotted as blue filled squares in Figure 6b. As we speculated, the 3D structures of the peptidomimetics distributed diversely along the PC1 and PC2 axes to mimic both main-chain and side-chain conformations of the various tetrapeptide motifs in PepX. The *cis*-folded scaffolds (**IV** and ***ent*-IV**) had low PC1 values to mimic the folded conformations, such as β-turns, while the *trans*-extended scaffolds (**II** and ***ent*-II**) and the *cis*-extended scaffolds (**III** and ***ent*-III**) had high PC1 values to mimic the extended conformations, such as β-strands, of the main chain of the tetrapeptide motifs. In addition, the *trans*-folded scaffolds (**I** and ***ent*-I**), which had middle PC1 values, mimic the main-chain conformations between β-turns and β-strands. The PC2 values of the eight scaffolds differed from each other, indicating that the two side chains (R^{i+1} and R^{i+2}) are oriented in different and diverse 3D positions. These analyses demonstrated that the cyclopropane-based peptidomimetics cover the spatial arrangement of the side chains differently, even when the main-chain conformations of the mimetics are analogous.

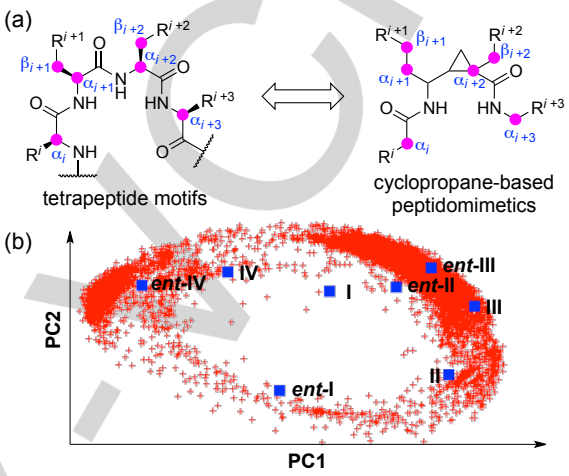

Figure 6. (a) The six carbon atoms are indicated by the magenta points, which were selected to build the chemical space. (b) Tetrapeptide motifs in PepX (red crosses) and X-ray structures of cyclopropane-based peptidomimetic scaffolds **I**–**IV** and ***ent*-I**–**IV** (blue filled squares) in the chemical space based on the 3D coordinates of the selected six carbon atoms. The horizontal axis and vertical axis represent PC1 and PC2, respectively.

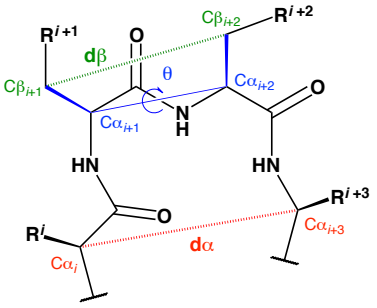

Figure 7. Descriptors for the peptide secondary structures (dα, dβ, θ).

Conformational Analysis-Driven Ligand Optimization

1) Identification of the Lead Stereoisomer

In a previous study,[13] the eight stereoisomers were designed as MCR ligands based on the tetrapeptide sequence (His[6]-L/D-Phe[7]-Arg[8]-Trp[9]), which is known as the core sequence of peptidic MCR ligands.[18] Among them, down/*trans*-folded mimetic **4** and down/*trans*-extended mimetic **5** (Figure 8a) showed definite affinity for the human MCR subtype 4 (hMC4R). Because the

two mimetics showed similar binding affinity for hMC4R (**4**, K_i = 0.38 μM; **5**, K_i = 0.37 μM), however, it was required to determine which of these mimetics could be the lead stereoisomer for further ligand optimization.

Based on the above-mentioned conformational analyses, stereoisomers **4** and **5** should be apart in the chemical space (corresponding to ***ent*-I** and ***ent*-II**, respectively, in Figure 6b), due to the distinct backbone conformation and side-chain positioning. As depicted in Figure 8a, the two mimetics are opposite at the C1' stereochemistry, and thus the 3D orientations of the *i* and *i*+1 moieties are differently constrained due to the strong cyclopropylic strain effect, as determined by the calculations (Figure 4) and X-ray crystal structures (Figure 5). We speculated that the two functional groups of the *i* and *i*+1 moieties, i.e., the imidazolyl and phenyl groups, in mimetics **4** and **5** might be ambiguously recognized by the receptor, as both are planar aromatic rings with π-binding ability tethered via a conformationally flexible "-CH_2-CH_2-" chain (indicated with dotted blue circles in Figure 8a). Therefore, to provide more conformational rigidity, we designed down/*trans*-folded mimetics **6**, **8**, and **10** (derivatives of **4**) and down/*trans*-extended mimetics **7**, **9**, and **11** (derivatives of **5**), in which the phenethyl group was shortened to a benzyl group and/or an AcNH- group was introduced at the *i* moiety (Figure 8b).

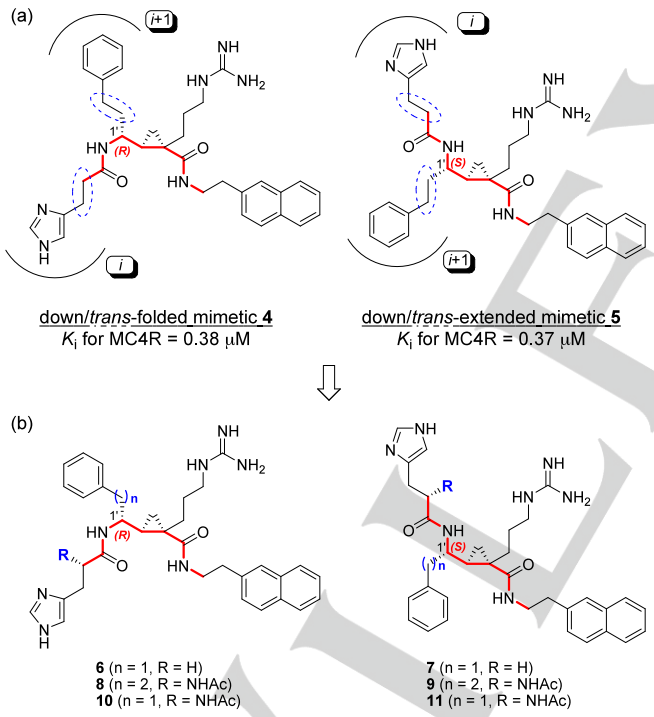

Figure 8. (a) Diagram of the structural difference between mimetics **4** and **5**. (b) Designed mimetics **6**-**11**, which are modified at the conformationally flexible methylene chains of **4** and **5** indicated with dotted blue circles.

The synthetic scheme for the modified mimetics **6**-**11** is shown in Scheme 2. The benzyl group was introduced by a diastereoselective Grignard reaction[19] to chiral *N*-*tert*-butylsulfinyl imines **12** and **13**. The diastereoselectivity and yield were sufficient under normal conditions (0.1 M substrate concentration at rt). This observation was in contrast to the same reaction with $PhCH_2CH_2MgCl$, in which a low concentration and high temperature (0.01 M at 110 ºC) were effective, and only low yield (30%) was produced when the substrate was **13**.[13] The major Grignard adducts were deprotected with HCl/AcOEt, followed by coupling with carboxylic acid **20** or **21**. The resulting crude amides were treated with K_2CO_3/MeOH. For the synthesis of **24**-**27**, the Fmoc group was exchanged with an Ac group in one-pot by the addition of excess amounts of Ac_2O after treatment with K_2CO_3 in MeOH (condition B). The primary hydroxyl group of **22**-**27** was converted to a guanidino group to give the desired compounds **6**-**11**.

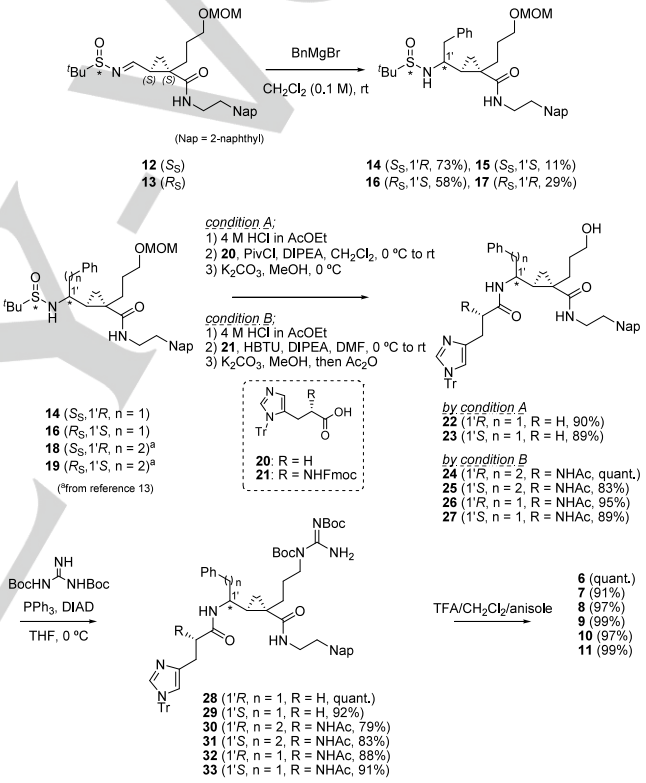

Scheme 2. Synthetic scheme for modified mimetics **6**-**11**.

All of the newly synthesized mimetics were evaluated for their binding affinity for hMC4R, and the results are summarized in Table 1. Unfortunately, the binding affinities for hMC4R of these modified mimetics were lower than those of the parent mimetics **4** and **5**. The difference in the affinities between each epimeric pair (**6** vs. **7**, **8** vs. **9**, and **10** vs. **11**), however, was larger than that between the parent epimeric pair **4** and **5**, as expected. In these three epimeric pairs, the down/*trans*-folded mimetics derived from **4** were significantly more potent than the corresponding down/*trans*-extended mimetics (K_i values: **6** < **7**,

8 < **9**, **10** < **11**). These results showed that the down/*trans*-folded structure is more preferable for binding to hMC4R, whose turn-like, but relatively extended, form could effectively mimic the conformation of the core tetrapeptide sequence (His-L/D-Phe-Arg-Trp) in its interaction with the receptor.

Table 1. Binding affinities of the modified mimetics **6**–**11** for hMC4R.

mimetic	scaffold	K_i (μM)[a]
6	down/*trans*-folded	1.70 ± 0.11
7	down/*trans*-extended	3.57 ± 0.07
8	down/*trans*-folded	0.64 ± 0.17
9	down/*trans*-extended	1.57 ± 0.19
10	down/*trans*-folded	4.00 ± 0.33
11	down/*trans*-extended	6.89 ± 0.66

[a] Mean value ± S.E. (n = 3).

2) Development of More Potent and Selective ligands

Based on the identification of the down/*trans*-folded mimetic **4** as the lead stereoisomer, the development of more potent ligands was investigated. Capping the terminal amino group of the tetrapeptide MCR ligand (H-His-D-Phe-Arg-Trp-NH_2) with a hydrophobic group increased the binding affinity for the MCR subtypes,[20] suggesting that a hydrophobic pocket existed around the MCR binding site of the terminal amino group of the core sequence. Therefore, if the down/*trans*-folded structure mimics the receptor-binding conformation of the core sequence, introducing a hydrophobic group onto the *i* moiety of **4** would increase the MCR binding affinity, hopefully with higher subtype selectivity. Accordingly, derivatives **34**-**36** with an N-terminal hydrophobic group were designed (Figure 9) and synthesized following the analogous procedure for the synthesis of **8** with the use of the corresponding carboxylic anhydride instead of Ac_2O at the K_2CO_3/MeOH treatment step.

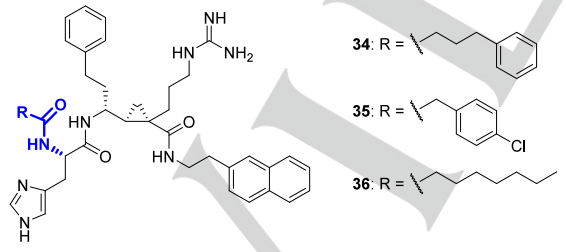

Figure 9. Designed mimetics **34**-**36** with a hydrophobic group at the N-terminal moiety.

The binding affinities for the three MCR subtypes (hMC3R, hMC4R, and hMC5R) are shown in Table 2. As expected, the binding affinity for the three subtypes increased in all mimetics except for **36** at hMC3R. Among them, mimetic **34** had the highest affinity for hMC4R (K_i = 0.032 μM), which was 10 times as potent as the lead **4**. As is the case with mimetic **4**, mimetic **34** showed antagonistic activity to hMC4R (IC_{50} = 0.22 μM), which was also approximately 10 times more potent. In addition, **34** appeared to be highly selective for hMC4R; the selectivity indices of hMC3R/hMC4R and hMC5R/hMC4R were 36 and 28, respectively, while those of **4** were 13 and 5.5. The stability of the mimetic **34** in human serum at 37 ºC was also tested, as the additional amide moiety might have made it susceptible to proteolysis. As a result, **34** had high proteolytic stability (93% remained after 24-h incubation), compared to the core sequence tetrapeptide, Ac-His-Phe-Arg-Trp-NH_2 ($t_{1/2}$ < 1 h).

Table 2. Effect of mimetics **34**–**36** for hMC3R, hMC4R, and hMC5R.

mimetic	K_i (μM)[a]			IC_{50} (μM)[c]
	hMC3R	hMC4R	hMC5R	hMC4R
4	4.90 ± 0.27	0.38 ± 0.05	2.09 ± 0.11	34% at 1μM 98% at 10μM
34	1.16 ± 0.11	0.032 ± 0.001	0.894 ± 0.288	0.22
35	0.77 ± 0.08	0.138 ± 0.024	0.233 ± 0.012	nd
36	50.7%[b]	0.235 ± 0.022	0.395 ± 0.037	nd

[a] Mean value ± S.E. (n = 3). [b] Inhibition rate of ^{125}I-labeled [Nle^4,D-Phe^7]-α-MSH binding at 10 μM. [c] Inhibitory effect on the agonistic activity of 4.7 nM of MT-II. For mimetic **4**, inhibition rates at 1 μM and 10 μM are shown. nd, not determined.

Discussion

A combination of computer-aided and organic synthesis-aided methods was applied to conformational analysis in this study. In the computational calculations (Figure 4) and X-ray crystallography (Figure 5), the backbone conformations of the mimetics were assessed based on the dα value to show their high diversity spanning folded to extended forms. The distance between α-carbons is easy to calculate and often used in structural studies of peptides and peptidomimetics;[4] however, it only describes the folded/extended character of the main-chain conformation. Although the main-chain conformation is important, it is essential to estimate the 3D positioning of the side chains, which often play a major role in the interaction with target molecules.

To estimate the side-chain positioning, Garland and Dean used the Cα-Cβ bond vector as a descriptor.[14c] While it is an

excellent descriptor, it is not easy to use a vector parameter to evaluate the structural analogy between a peptidomimetic scaffold and a peptide secondary structure. Instead, Burgess *et al*. used the distance between the atoms corresponding to Cβ as a scalar descriptor,[14b] which is presented as dβ in our study. Because dβ does not reflect the orientation of the side chains, however, it works as a "rough cut" parameter, as stated in their paper.[14b] Therefore, an alternative analysis was required for more accurate fitting of the 3D positioning of the side chains.

We used PCA to generate the desired parameters correlating with the structural information of both the main chain and side chains (Figure 6). PC2 was moderately correlated with the θ value; therefore, the 3D positioning of side chains with similar dβ values can be evaluated separately depending on the θ value, which indicates the orientation of the side chains. Notably, as depicted in Figure 10, side chains R^{i+1} and R^{i+2} in the cyclopropane-based peptidomimetics are oriented opposite from each other in space in the enantiomeric pairs, i.e., the up-series vs. down-series, based on a combinational steric effects of the *cis/trans*-restriction and the cyclopropylic strain. This 3D structural difference between the enantiomers leads to a variety of θ values, resulting in diversity along the PC2 axis and making it possible to mimic a wide range of spatial arrangements of tetrapeptide motifs in terms of the side-chain positioning.

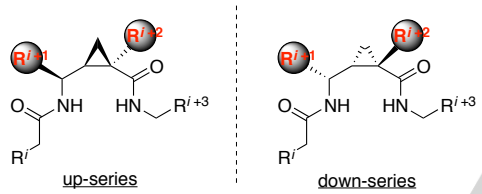

Figure 10. The opposite spatial arrangements of the side chains R^{i+1} and R^{i+2} between the up-series and down-series.

While the overall conformation is restricted, the 3D positions of the functional groups themselves showed some flexibility in the designed MCR ligands. This flexibility might have made the ligand-receptor interaction loose, as observed in **4** and **5**. The two mimetics showed similar binding affinity for hMC4R, despite having a distinct 3D structure. This contradiction was addressed by the conformational analysis-driven strategy (Figure 8). The methylene chains tethering R^i and R^{i+1} in **4** and **5** were modified to differentiate their interaction with the receptor, employing the strong cyclopropylic strain effect. As a result, it was indicated that the down/*trans*-folded mimetic **4** could mimic the receptor-binding conformation of the core sequence. Accordingly, mimetic **4** was successfully derivatized to the 10-times more potent hMC4R ligand **34** (K_i = 32 nM) with good subtype selectivity and proteolytic stability.

The mimetics **4** and **34** had antagonistic activity to hMC4R. This antagonistic activity can be explained by a difference of the 3D positions of the side-chain functional groups from those required for agonistic activity. The well-known peptidic MCR agonist MT-II[21] is converted to an antagonist by subtle structural changes, e.g., SHU9119 and SHU8941, in which the phenyl group of D-Phe[7] is replaced with a 2-naphthyl or *p*-iodophenyl group, respectively.[22] The conformations of MT-II and SHU-9119 are reportedly quite similar except for some difference in the 3D positions of the side-chain functional groups.[23] Interestingly, a single mutation of Leu^{133} to Met in hMC4R converts SHU9119 from an antagonist to an agonist without affecting its binding affinity.[24] Considering these functional fluctuations among peptidic MCR ligands, it can be deduced that the antagonistic activity of mimetics **4** and **34** is due to the 3D positions of the side-chain functional groups rather than the overall structure of the molecule. This is also supported by the effect of the introduction of an N-terminal hydrophobic group in **34**, which increased MCR binding affinity, as similarly observed in the peptidic MCR agonists.

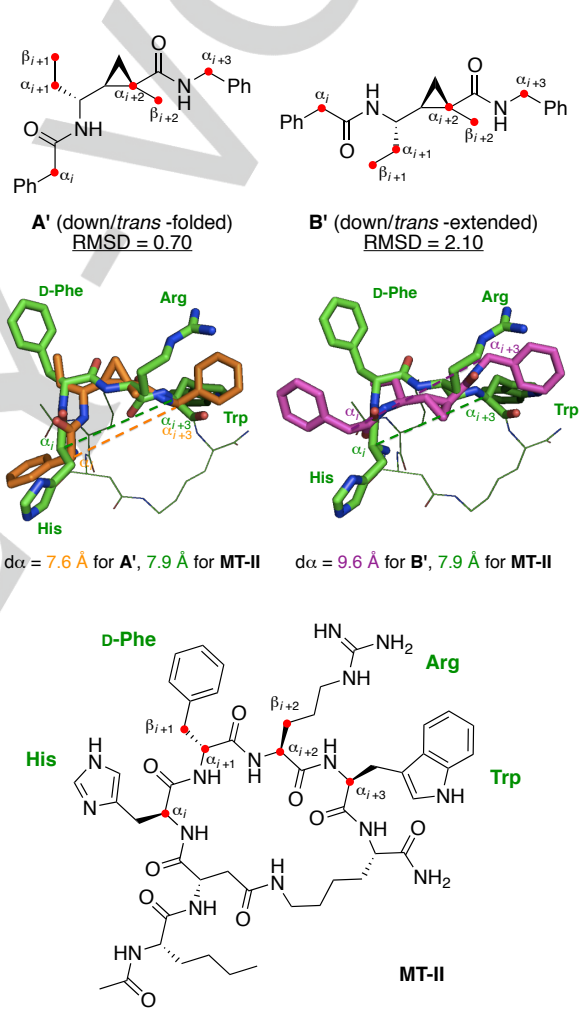

Figure 11. Superimposition of the reported conformation of MT-II (green) and the X-ray crystallographic structures of compounds **A'** (orange) and **B'** (magenta). The superimposing points for root-mean-square deviation (RMSD) calculations are $C\alpha_i$, $C\alpha_{i+1}$, $C\alpha_{i+2}$, $C\alpha_{i+3}$, $C\beta_{i+1}$, and $C\beta_{i+2}$ in MT-II and the corresponding carbons in compounds **A'** and **B'** (indicated by red points).

The information on the receptor-binding conformation of the core sequence obtained by our organic chemistry-based approach was indeed consistent with that obtained by an independent spectroscopic and computational approach. Carotenuto *et al* previously reported the NMR-based conformational calculations of MT-II.[23b] The X-ray crystal structures of the simplified mimetics **A'** and **B'** (corresponding to **4** and **5**, respectively) were superimposed on the calculated structure of the core sequence in MT-II. As depicted in Figure 11, the X-ray crystal structure of **A'** was well superimposed on the calculated MT-II structure with the almost same dα values, whereas that of **B'** was not. This difference was quantified by the root-mean-square deviation values calculated for $C\alpha_i$, $C\alpha_{i+1}$, $C\alpha_{i+2}$, $C\alpha_{i+3}$, $C\beta_{i+1}$, and $C\beta_{i+2}$ in MT-II and the corresponding carbon atoms in **A'** and **B'** (indicated by red points in Figure 11), which were 0.70 for **A'** and 2.10 for **B'**, respectively. The 3D structures of our peptidomimetics were also compared with the reported low-energy conformations of MT-II[23b] in the chemical space based on PC1 and PC2. As shown in Figure 12, the plots for the low-energy conformations of the core sequence in MT-II (green squares) distributes near the plot for the scaffold ***ent*-I** rather than that for scaffold ***ent*-II**. These results support that the down/*trans*-folded structure of **4**, identified as the lead stereoisomer, would be similar to the conformation of the core sequence in MT-II from the viewpoint of both the main-chain conformation and the side-chain positioning.[25]

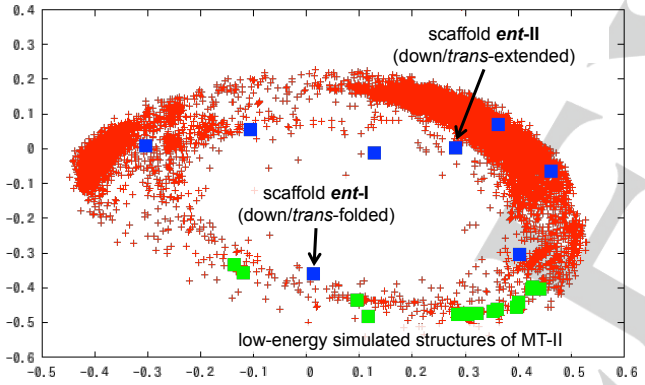

Figure 12. Comparison of the cyclopropane-based peptidomimetics with the NMR-based calculated conformations of the core sequence in MT-II in the chemical space. x-axis, PC1; y-axis, PC2; green squares, the low-energy simulated conformations of the core sequence in MT-II; blue squares, the eight scaffolds of the cyclopropane-based peptidomimetics; red crosses, tetrapeptide motifs in the PepX database.

The comparison in the chemical space (Figure 12) also visualizes how the 3D structural diversity-oriented strategy worked to identify ***ent*-I** as a lead scaffold. Because the secondary structure around the core sequence in the peptidic MCR ligands is thought to be a β-turn,[18] a peptidomimetic strategy targeting MCRs often focuses on β-turn mimetic scaffolds,[26] as typically used for GPCR-targeting peptidomimetics.[5] It is unclear, however, whether the core tetrapeptide sequence itself forms the β-turn. For example, two different calculated models on the β-turn structure were used for the linear peptidic MCR ligand, NDP-MSH,[27] i.e., type II' β-turn composed of the core sequence itself (His^6-D-Phe^7-Arg^8-Trp^9)[28] and type I' β-turn composed of the tetrapeptide shifted from the core sequence by one residue (Glu^5-His^6-D-Phe^7-Arg^8).[29] The PC1 value of MT-II distributes in the middle to high range, supporting that the conformation of the core sequence would be relatively extended rather than forming a β-turn structure. Therefore, an effective peptidomimetic backbone targeting the MCRs could be extended or halfway between the folded and the extended forms. This atypical preference for the extended conformation might have been covered by the PC1 diversity of the cyclopropane-based peptidomimetics, resulting in the identification of the turn-like but more extended structure (halfway between the folded and the extended forms) of ***ent*-I**. The negative PC2 value of MT-II is mainly attributed to the D-configuration of the D-Phe^7 residue. The D-Phe^7 residue is important for the increased MCR affinity of many peptidic MCR ligands, including MT-II and NDP-MSH. Thus, this unique side-chain positioning arising from the D-configuration was covered by the PC2 diversity of the designed mimetics.

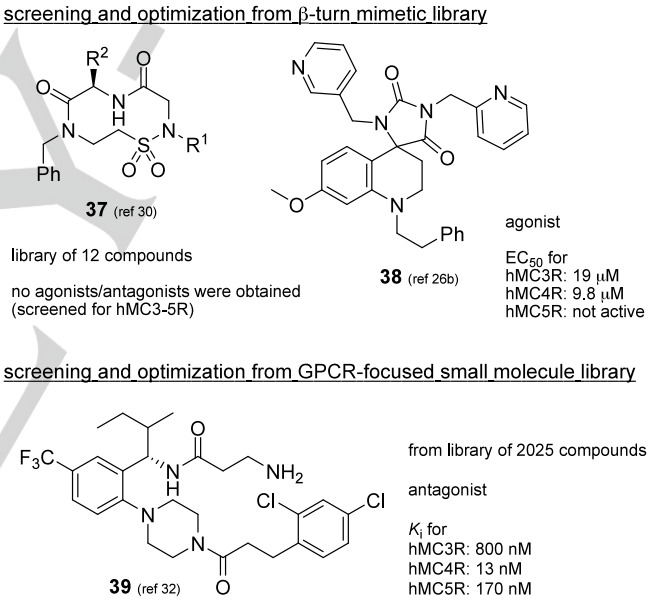

Figure 13. Examples of other approaches to obtain MCR ligands.

Examples of MCR ligands obtained by other approaches are shown in Figure 13. There are several reports focusing on β-turn mimetics. Although successful examples such as **38** were reported,[26b] the potency and subtype selectivity were not high, and β-turn mimetic scaffold **37** was not so effective to obtain MCR ligands.[30] These results might be due to the preference of MCRs for extended conformation of peptidomimetics as described above. As another strategy different from peptidomimetics, high-throughput screening of a GPCR-focused small molecule library (2025 compounds)[31] and following

optimization developed hMC4R antagonist **39**.[32] Its potency and subtype selectivity are comparable to those of **34**, indicating that the only eight stereoisomers designed in this study could work as effectively as such larger library.

Conclusions

Focusing on the importance of the 3D structural diversity of molecules in searching for and mimicking a key conformation, computational calculations and X-ray crystallography confirmed that the steric and stereoelectronic features of cyclopropane work effectively to constrain the peptidomimetic molecules into diverse 3D structures. This 3D structural diversity was depicted by the PCA, which showed that the cyclopropane-based peptidomimetics cover the broad chemical space filled by peptide secondary structures in terms of both main-chain and side-chain conformations. These detailed conformational analyses allowed us to obtain the 3D structural information that is important for rational ligand optimization. As a result, down/*trans*-folded mimetic **4** was selected, leading to more potent and subtype-selective MCR ligand **34**. The process described in this study was carried out without knowing the 3D structural information of the target and its peptide ligands. Therefore, this peptidomimetic strategy can be applied even when the ligand-target interaction is poorly documented, as is often the case in the early stage of drug development.

Acknowledgements

We are grateful to Prof. Dr. A. Carotenuto (University of Naples) for providing the calculated structural data of MT-II and also to Sanyo Fine Co., Ltd. for the gift of the chiral epichlorohydrins. This investigation was supported by Grant-in-Aids for Scientific Research (21390028 to S.S. and 2310550201, 2179000300 to M.A.) from the Japan Society for the Promotion of Science.

Keywords: Peptidomimetics • Drug design • Three-dimensional structural diversity • Chemical space • Conformation analysis

[1] I. Avan, C. D. Hall, A. R. Katritzky, *Chem. Soc. Rev.* **2014**, *43*, 3575-3594.

[2] R. M. J. Liskamp, D. T. S. Rijkers, J. A. W. Kruijtzer, J. Kemmink, *ChemBioChem* **2011**, *12*, 1626-1653.

[3] a) D. Chatenet, B. Folch, D. Feytens, M. Létourneau, D. Tourwé, N. Doucet, A. Fournier, *J. Med. Chem.* **2013**, *56*, 9612-9622; b) L. Karhu, A. Turku, H. Xhaard, *BMC Struct. Biol.* **2015**, *15*, 9.

[4] L. R. Whitby, Y. Ando, V. Setola, P. K. Vogt, B. L. Roth, D. L. Boger, *J. Am. Chem. Soc.* **2011**, *133*, 10184-10194.

[5] G. Ruiz-Gómez, J. D. A. Tyndall, B. Pfeiffer, G. Abbenante, D. P. Fairlie, *Chem. Rev.* **2010**, *110*, PR1-PR41.

[6] R. Haubner, D. Finsinger, H. Kessler, *Angew. Chem. Int. Ed. Engl.* **1997**, *36*, 1374-1389.

[7] K. C. Chou, *Anal. Biochem.* **2000**, *286*, 1-16.

[8] a) M. A. Ceruso, D. F. McComsey, G. C. Leo, P. Andrade-Gordon, M. F. Addo, R. M. Scarborough, D. Oksenberg, B. E. Maryanoff, *Bioorg. Med. Chem.* **1999**, *7*, 2353-2371; b) S. Luca, J. F. White, A. K. Sohal, D. V. Filippov, J. H. van Boom, R. Grisshammer, M. Baldus, *Proc. Natl. Acad. Sci. USA* **2003**, *100*, 10706-10711.

[9] a) P. D. Armstrong, J. G. Cannon, J. P. Long, *Nature* **1968**, *220*, 65-66; b) K. Shimamoto, Y. Ohfune, *J. Med. Chem.* **1996**, *39*, 407-423; c) T. Onishi, C. Mukai, R. Nakagawa, T. Sekiyama, M. Aoki, K. Suzuki, H. Nakazawa, N. Ono, Y. Ohmura, S. Iwayama, M. Okunishi, T. Tsuji, *J. Med. Chem.* **2000**, *43*, 278-282; d) K. Vervisch, M. D'hooghe, K. W. Tornroos, N. De Kimpe, *Org. Biomol. Chem.* **2009**, *7*, 3271-3279; e) K. Yoshida, K. Yamaguchi, A. Mizuno, Y. Unno, A. Asai, T. Sone, H. Yokosawa, A. Matsuda, M. Arisawa, S. Shuto, *Org. Biomol. Chem.* **2009**, *7*, 1868-1877; f) H. Zhang, W. Tückmantel, J. B. Eaton, P.-w. Yuen, L.-F. Yu, K. M. Bajjuri, A. Fedolak, D. Wang, A. Ghavami, B. Caldarone, N. E. Paterson, D. A. Lowe, D. Brunner, R. J. Lukas, A. P. Kozikowski, *J. Med. Chem.* **2012**, *55*, 717-724; g) M. Boztaş, Y. Çetinkaya, M. Topal, İ. Gülçin, A. Menzek, E. Şahin, M. Tanc, C. T. Supuran, *J. Med. Chem.* **2015**, *58*, 640-650.

[10] a) K. I. Varughese, C. H. Wang, H. Kimura, C. H. Stammer, *Int. J. Pept. Protein Res.* **1988**, *31*, 299-300; b) K. Burgess, K.-K. Ho, B. Pal, *J. Am. Chem. Soc.* **1995**, *117*, 3808-3819; c) P. Wipf, J. Xiao, *Org. Lett.* **2005**, *7*, 103-106; d) J. E. DeLorbe, J. H. Clements, M. G. Teresk, A. P. Benfield, H. R. Plake, L. E. Millspaugh, S. F. Martin, *J. Am. Chem. Soc.* **2009**, *131*, 16758-16770; e) S. S. Bhella, M. Elango, M. P. S. Ishar, *Tetrahedron* **2009**, *65*, 240-246; f) L. Sernissi, M. Petrović, D. Scarpi, A. Guarna, A. Trabocchi, F. Bianchini, E. G. Occhiato, *Chem. Eur. J.* **2014** *20*, 11187-11203.

[11] a) Y. Kazuta, H. Abe, T. Yamamoto, A. Matsuda, S. Shuto, *J. Org. Chem.* **2003**, *68*, 3511-3521; b) A. J. Cruz-Cabeza, F. H. Allen, *Acta Crystallogr. Sect. B: Struct. Sci.* **2011**, *67*, 94-102.

[12] a) S. Shuto, S. Ono, Y. Hase, N. Kamiyama, H. Takada, K. Yamashita, A. Matsuda, *J. Org. Chem.* **1996**, *61*, 915-923; b) M. Watanabe, T. Hirokawa, T. Kobayashi, A. Yoshida, Y. Ito, S. Yamada, N. Orimoto, Y. Yamasaki, M. Arisawa, S. Shuto, *J. Med. Chem.* **2010**, *53*, 3585-3593.

[13] A. Mizuno, S. Miura, M. Watanabe, Y. Ito, S. Yamada, T. Odagami, Y. Kogami, M. Arisawa, S. Shuto, *Org. Lett.* **2013**, *15*, 1686-1689.

[14] Methods for defining peptidomimetic structure have been reported. For example, a) using distance between Cα atoms, U. Rosenström, C. Sköld, B. Plouffe, H. Beaudry, G. Lindeberg, M. Botros, F. Nyberg, G. Wolf, A. Karlén, N. Gallo-Payet, A. Hallberg, *J. Med. Chem.* **2005**, *48*, 4009-4024; b) using distance between Cβ atoms, E. Ko, J. Liu, K. Burgess, *Chem. Soc. Rev.* **2011**, *40*, 4411-4421; c) using Cα-Cβ bond vector, S. L. Garland, P. M. Dean, *J. Comput. Aided Mol. Des.* **1999**, *13* 485-498; d) using dihedral angle, P. Gillespie, J. Cicariello, G. L. Olson, *Biopolymers* **1997**, *43*, 191-217. For recent review of the classification of peptidomimetics, e) M. Pelay-Gimeno, A. Glas, O. Koch, T. N. Grossmann, *Angew. Chem. Int. Ed.* **2015**, *54*, 8896-8927.

[15] For the synthesis of compounds **A'-D'**, see Supporting Information. The supplementary crystallographic data in CIF format can be obtained from The Cambridge Crystallographic Data Centre via http://www.ccdc.cam.ac.uk/products/csd/request/ with the CCDC numbers: CCDC 865592, CCDC 865593, CCDC 865594 and CCDC 865595.

[16] a) C. M. Dobson, *Nature* **2004**, *432*, 824-828; b) T. Kameda, S. Takada, *Proc. Natl. Acad. Sci. USA* **2006**, *103*, 17765-17770; c) J.-L. Reymond, M. Awale, *ACS Chem. Neurosci.* **2012**, *3*, 649-657.

[17] P. Vanhee, J. Reumers, F. Stricher, L. Baeten, L. Serrano, J. Schymkowitz, F. Rousseau, *Nucleic Acids Res.* **2010**, *38*, D545-D551.

[18] E. M. Haslach, J. W. Schaub, C. Haskell-Luevano, *Bioorg. Med. Chem.* **2009**, *17*, 952-958.

[19] M. T. Robak, M. A. Herbage, J. A. Ellman, *Chem. Rev.* **2010**, *110*, 3600-3740.

[20] a) L. N. Koikov, F. H. Ebetino, M. G. Solinsky, D. Cross-Doersen, J. J. Knittel, *Bioorg. Med. Chem. Lett.* **2003**, *13*, 2647-2650; b) J. R. Holder, F. F. Marques, Z. Xiang, R. M. Bauzo, C. Haskell-Luevano, *Eur. J. Pharmacol.* **2003**, *462*, 41-52; c) L. N. Koikov, F. H. Ebetino, M. G.

Solinsky, D. Cross-Doersen, J. J. Knittel, *Bioorg. Med. Chem. Lett.* **2004**, *14*, 3997-4000.
[21] F. Al-Obeidi, M. E. Hadley, B. M. Pettitt, V. J. Hruby, *J. Am. Chem. Soc.* **1989**, *111*, 3413-3416.
[22] V. J. Hruby, D. S. Lu, S. D. Sharma, A. L. Castrucci, R. A. Kesterson, F. A. Alobeidi, M. E. Hadley, R. D. Cone, *J. Med. Chem.* **1995**, *38*, 3454-3461.
[23] a) M. Cai, C. Cai, A. V. Mayorov, C. Xiong, C. M. Cabello, V. A. Soloshonok, J. R. Swift, D. Trivedi, V. J. Hruby, *J. Peptide Res.* **2004**, *63*, 116-131; b) P. Grieco, D. Brancaccio, E. Novellino, V. J. Hruby, A. Carotenuto, *Eur. J. Med. Chem.* **2011**, *46*, 3721-3733.
[24] Y. Yang, M. Chen, Y. Lai, I. Gantz, K. E. Georgeson, C. M. Harmon, *J. Biol. Chem.* **2002**, *277*, 20328-20335.
[25] The plot for up/*trans*-extended scaffold **II** is also close to the plots for MT-II in the chemical space (Figure 12). However, more detailed conformational analysis showed that **II** occupied an area apart from MT-II, while the area occupied by ***ent*-I** significantly overlapped with that by MT-II. For details, see section VII and Figure S6 in Supporting Information.
[26] a) C. Haskell-Luevano, A. Rosenquist, A. Souers, K. C. Khong, J. A. Ellman, R. D. Cone, *J. Med. Chem.* **1999**, *42*, 4380-4387; b) T. R. Webb, L. Jiang, S. Sviridov, R. E. Venegas, A. V. Vlaskina, D. McGrath, J. Tucker, J. Wang, A. Deschenes, R. Li, *J. Comb. Chem.* **2007**, *9*, 704-710.
[27] T. K. Sawyer, P. J. Sanfilippo, V. J. Hruby, M. H. Engel, C. B. Heward, J. B. Burnett, M. E. Hadley, *Proc. Natl. Acad. Sci. USA* **1980**, *77*, 5754-5758.
[28] K. L. Chapman, G. K. Kinsella, A. Cox, D. Donnelly, J. B. C. Findlay, *J. Mol. Biol.* **2010**, *401*, 433-450.
[29] M.-K. Cho, C.-J. Lee, C.-H. Lee, S.-Z. Li, S.-K. Lim, J.-H. Baik, W. Lee, *J. Struct. Biol.* **2005**, *150*, 300-308.
[30] B. Wels, J. A. W. Kruijtzer, K. M. Garner, R. A. H. Adan, R. M. J. Liskamp, *Bioorg. Med. Chem. Lett.* **2005**, *15*, 287-290.
[31] K. Lavrador, B. Murphy, J. Saunders, S. Struthers, X. Wang, J. Williams, *J. Med. Chem.* **2004**, *47*, 6864-6874.
[32] W. Jiang, F. C. Tucci, C. W. Chen, M. Arellano, J. A. Tran, N. S. White, D. Marinkovic, J. Pontillo, B. A. Fleck, J. Wen, J. Saunders, A. Madan, A. C. Foster, C. Chen, *Bioorg. Med. Chem. Lett.* **2006**, *16*, 4674-4678.

10.1002/chem.201605312

WILEY-VCH

FULL PAPER

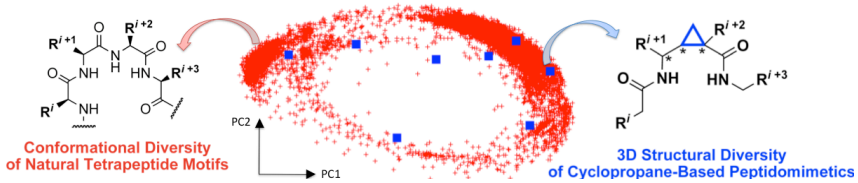

Detailed conformational analyses revealed that cyclopropane provides conformationally restricted peptidomimetics with high three-dimensional (3D) structural diversity, mimicking broad peptide secondary structures. The presented strategy is effective not only for designing non-peptidic ligands, but also for rational optimization of these ligands based on the plausible target-binding conformation without requiring the 3D structural information of the target and its peptide ligands.

*Akira Mizuno, Tomoshi Kameda, Tomoki Kuwahara, Hideyuki Endoh, Yoshihiko Ito, Shizuo Yamada, Kimiko Hasegawa, Akihito Yamano, Mizuki Watanabe, Mitsuhiro Arisawa and Satoshi Shuto**

Cyclopropane-Based Peptidomimetics Mimicking Wide-Ranging Secondary Structures of Peptides: Conformational Analysis and Their Use in Rational Ligand Optimization